Proceedings of the ASME 2024
International Mechanical Engineering Congress and Exposition
IMECE2024
November 17-21, 2024, Portland, OR

IMECE2024-145441

INVESTIGATING SEISMOCARDIOGRAM PATTERNS: A COMPUTATIONAL MODELING OF CARDIAC WALL MOTION PROPAGATION TO THE CHEST SURFACE

Mohammadali Monfared[1], Peshala Thibbotuwawa Gamage[2], Amirtaha Taebi[1,*]

[1]Mississippi State University, Mississippi State, MS
[2]Florida Institute of Technology, Melbourne, FL

ABSTRACT

Cardiovascular diseases, the leading cause of global mortality, demand refined diagnostic methods. Seismocardiography (SCG), a noninvasive method of measuring cardiovascular-induced vibrations on the chest surface, offers promise in assessing cardiac function. The cardiac wall movements are transmitted to the organs around the heart and eventually damped onto the chest surface, where they manifest as visible vibrations. These chest surface vibrations can be measured using an accelerometer via SCG. Although SCG signals are widely used in literature, further investigations are needed to understand the genesis of their patterns under different pathophysiological conditions. The goal of this study is to improve our understanding of the origin of SCG signals by simulating the transmission of cardiac motion reaching the chest surface using finite element method, and linking back the patterns of the simulated SCG signals to specific cardiac events. The computational domain, extracted from 4D computed tomography (CT) images of a healthy subject, comprised the lungs, ribcage, and chest muscles and fat. Using the Lukas-Kanade algorithm, the cardiac wall motion was extracted from the 4D CT scan images and was used as a displacement boundary condition. The elastic material properties were assigned to the lungs, muscles, fat, and rib cage. The dorsoventral SCG component from the finite element modeling was compared with two actual SCG signals obtained from the literature. The left ventricular volume was also calculated from the CT scans and was used to interpret the SCG waveforms. Important cardiac phases were labeled on the SCG signal extracted from the computationally modeled acceleration map near the xiphoid. This type of analysis can provide insights into various cardiac parameters and SCG patterns corresponding to the mitral valve closing, mitral valve opening, aortic valve opening, and aortic valve closure. These findings suggested the effectiveness of this modeling approach in understanding the underlying sources of the SCG waveforms.

*Corresponding author: ataebi@abe.msstate.edu

Keywords: Seismocardiography, finite element modeling, cardiac mechanics, cardiac vibrations

NOMENCLATURE

Equation terms

f	Force [N]
M	Mass matrix [kg]
C	Damping matrix [kg s^{-1}]
K	Stiffness matrix [N m^{-1}]
$\ddot{x}$	Acceleration [m s^{-2}]
$\dot{x}$	Velocity [m s^{-1}]
x	Displacement [m]

Medical terms

SCG	Seismocardiography
ECG	Electrocardiography
FE	Finite element
CT	Computed tomography
AC	Aortic valve closure
AO	Aortic valve opening
MC	Mitral valve closure
MO	Mitral valve opening
CVD	Cardiovascular disease
LV	Left ventricle

1. INTRODUCTION

The 2013-2018 National Health and Nutrition Examination Survey and the 2020 U.S. Census project a significant rise in the prevalence of the cardiovascular diseases (CVDs) from 2025 to 2060. During this period, the combined prevalence of ischemic heart disease, heart failure, myocardial infarction, and stroke combined is expected to increase by 17.4 million cases, highlighting the critical need for more robust and accurate cardiac monitoring methods [1–7]. Cardiovascular monitoring can be performed using both invasive and noninvasive techniques. Invasive methods typically require clinical settings and are often expensive. In contrast, noninvasive methods, such as electrocardiography (ECG), allow for remote monitoring of cardiovascular

health outside of clinical environments [8, 9]. While ECG provides information on the electrical activity of heart [10], seismocardiography (SCG) is another noninvasive method that detects chest surface vibrations, primarily originating from the heart's mechanical functions, including pericardial motion, valve activity, and alterations in blood momentum [11–15]. SCG can also be described as the acceleration response to the heartbeat, with waveforms originating from either the heart or the blood flow in major arteries [10]. This technique has shown promise for diagnosing and monitoring various cardiac conditions and offering complementary information to ECG and other noninvasive cardiac monitoring methods [11].

The signal obtained from SCG on the chest surface is believed to originate from the three-dimensional motion of the heart during the cardiac cycle. The complexity of these heart motions, combined with vibrations generated by blood flow and valve activity, poses challenges in interpreting SCG patterns and identifying their vibrational sources [16]. To address this, Crow *et al.* (1994) and Giorgis *et al.* (2008) attempted to correlate specific fiducial points in the SCG signal with the timing of corresponding cardiac events observed in medical imaging [17, 18]. In a more recent study, Mann *et al.* (2024) investigated how measuring SCG signals from various chest locations affects the estimation of cardiac time intervals and other SCG fiducial points [19]. Their findings highlighted the significance of SCG signal variations on the chest surface and their impact on the interpretation of the SCG patterns and their underlying physiological sources, such as detecting aortic valve opening based on the SCG signal. In this context, finite element (FE) modeling offers a valuable approach for identifying the origins of SCG signals. Patient-specific FE models, developed using precise input parameters and constraints obtained from medical imaging and personalized data, can shed light on SCG patterns and their variations under different pathophysiological conditions [20].

FE modeling of cardiovascular-generated vibrations can be conducted using both 2D and 3D representations. While 2D modeling provides a simplified view of cardiac vibration propagation to the chest, 3D models offer a more detailed and accurate picture of these vibrations and overall cardiac function. Gamage *et al.* (2019)[20] utilized a 2D computational model to simulate SCG signals, using cardiac wall motion as the inlet boundary condition. The results indicated that the model could replicate key features observed in SCG waveforms, offering potential insights into SCG signal generation, and suggesting future validation and extensions to 3D modeling using ECG-gated cardiac magnetic resonance (MR) or computed tomography (CT) scans. In a subsequent study, Gamage [21] developed a 3D model to measure chest surface vibrations associated with cardiac activity. This model employed medical imaging reconstruction and FE simulations to investigate the transmission of myocardial motion to the chest surface, establishing a correlation between heart muscle activity and SCG signals. The study's findings suggested that specific cardiac events, such as aortic valve opening (AO) and closure (AC) and mitral valve opening (MO), could be determined using the modeled SCG signal. Akhbardeh *et al.* (2009) [10] investigated SCG and its relationship with cardiac events using a FE electromechanical model based on diffusion tensor MR data. Their FE model of the heart, which considered its mechanical behavior throughout the cardiac cycle—including aspects such as contraction, relaxation, and blood flow dynamics—allowed them to calculate SCG waveforms and identify key fiducial points. Sandler *et al.* (2023) [22] assessed the impact of increased soft tissue thickness on SCG signals and their relation with cardiac activities using SCG FE modeling. Gurev *et al.* (2012) [12] developed a 3D FE electromechanical canine heart model to replicate SCG signals. Their model successfully reproduced major SCG peaks and revealed that SCG signals capture the heart's pressure on the ribs. Experimental results from human volunteers showed that the SCG peak aligns with the maximum acceleration of blood in the aorta, and the first SCG peak after the ECG R-wave corresponds to AO. Their study showed that SCG peaks related to aortic valve events and blood acceleration result from ventricular contraction and changes in ventricle dimensions during blood ejection. Few studies have developed simplified numerical models for analyzing SCG signals in the presence of CVDs. For instance, Mithani *et al.* (2022) [23] created 3D models of infant hearts with single ventricle disease and compared the modeled SCG signals with gold-standard SCG signals acquired by wearable sensors to enhance understanding of SCG signal characteristics.

This study aims to establish a foundation for advanced, patient-specific FE analyses of SCG signals. We present an initial version of our image-based FE pipeline, demonstrated on a healthy human subject. The methodology employs the Lucas-Kanade algorithm to extract heart wall motion from 4D CT scan images (3D geometry + time), which serves as the input displacement for FE simulations. Our 3D computational domain incorporates key anatomical structures including the lungs, ribcage, chest muscles, and fat, all precisely segmented from CT images. The pipeline's output is a high-resolution, simulated vibration map of the chest surface. This approach integrates detailed anatomical data with sophisticated computational modeling, potentially enabling more accurate and personalized interpretations of SCG signals in clinical settings.

2. MATERIALS AND METHODS

2.1 Cardiac Motion Tracking with Optical Flow

This paper utilized 4D CT scan images of a healthy human subject from an online dataset to define a realistic computational domain and capture the cardiac wall motion throughout a cardiac cycle, which served as the input boundary condition for the computational model. The original 4D CT dataset consisted of 3D volumes at 10 time points during the cardiac cycle. To achieve a higher temporal resolution, twelve 3D volumes were interpolated between each pair of two consecutive time points, resulting in a sampling frequency of 120 Hz, assuming a cardiac cycle duration of 1 second.

A custom MATLAB implementation of the Lucas-Kanade optical flow algorithm [24] was developed to track the time-resolved displacements of the heart wall throughout a complete cardiac cycle. The Lucas-Kanade algorithm, introduced in 1981, is a fast image registration technique based on spatial intensity gradients, widely used for optical flow estimation and feature tracking in computer vision tasks. This approach solves optical flow equations to estimate pixel velocities, enabling the track-

ing of dynamic cardiac wall displacements in three dimensions. The resulting data provided displacement information for selected points along the pericardium, capturing the complex 3D motion of the heart during its pumping cycle.

Let (x, y, z) represent a point within the volumetric domain, which is a 3D geometry created by merging image slices along the short axis. Here, x and y correspond to the width and length of the images, while z represents the direction perpendicular to the images. If the intensity of a point at coordinates (x, y, z) at a specific time t is $I(x, y, z, t)$, and if that same point shifts to a new location $(x+\delta x, y+\delta y, z+\delta z)$ over a time interval δt (Figure 1), the optical flow method assumes that the intensity remains constant, as expressed in (1).

$$I(x, y, z, t) = I(x + \delta x, y + \delta y, z + \delta z, t + \delta t) \tag{1}$$

Applying a first-order Taylor series expansion to the right-hand side of (1) yields:

$$\begin{aligned} I(x + \delta x, y + \delta y, z + \delta z, t + \delta t) = I(x, y, z, t) \\ + \frac{\partial I}{\partial x}\delta x + \frac{\partial I}{\partial y}\delta y + \frac{\partial I}{\partial z}\delta z \\ + \frac{\partial I}{\partial t}\delta t + \mathcal{O}(\delta^2) \end{aligned} \tag{2}$$

Substituting (2) into (1) and neglecting higher-order terms results in:

$$\frac{\partial I}{\partial x}\frac{\delta x}{\delta t} + \frac{\partial I}{\partial y}\frac{\delta y}{\delta t} + \frac{\partial I}{\partial z}\frac{\delta z}{\delta t} = -\frac{\partial I}{\partial t} \tag{3}$$

This equation can be rewritten in a more compact form:

$$I_x V_x + I_y V_y + I_z V_z = -I_t \tag{4}$$

where I_x, I_y, I_z, and I_t represent the spatial and temporal partial derivatives of the intensity at (x, y, z), and V_x, V_y, and V_z represent the velocity components in the x, y, and z directions, respectively. The Lucas-Kanade method aims to determine the displacement vector for each small pixel patch by solving equation (4). This approach assumes that the motion between consecutive frames can be approximated by a 3D vector (u, v, w) that minimizes the difference between the observed spatial and temporal gradients.

2.2 Forced Vibration Model of Chest Surface Motion

Forced vibration occurs when a system oscillates under an external variable force or displacement. In this study, the heart is considered the primary source of chest surface vibrations. The cardiac wall motion, driven by the blood-pumping process, induces vibrations in surrounding body organs. The equation of motion is expressed as:

$$f(t) = [M]\ddot{x} + [C]\dot{x} + [K]x \tag{5}$$

where $f = Ku$ represents the force induced by the externally imposed displacement on the system. In (5), f is the vector of applied forces, $[M]$ is the mass matrix, $[C]$ is the damping matrix, $[K]$ is the stiffness matrix, $\ddot{x}$ is acceleration, $\dot{x}$ is velocity, and x is displacement. In time domain analysis, both the stiffness matrix K and force vector f vary with time, necessitating

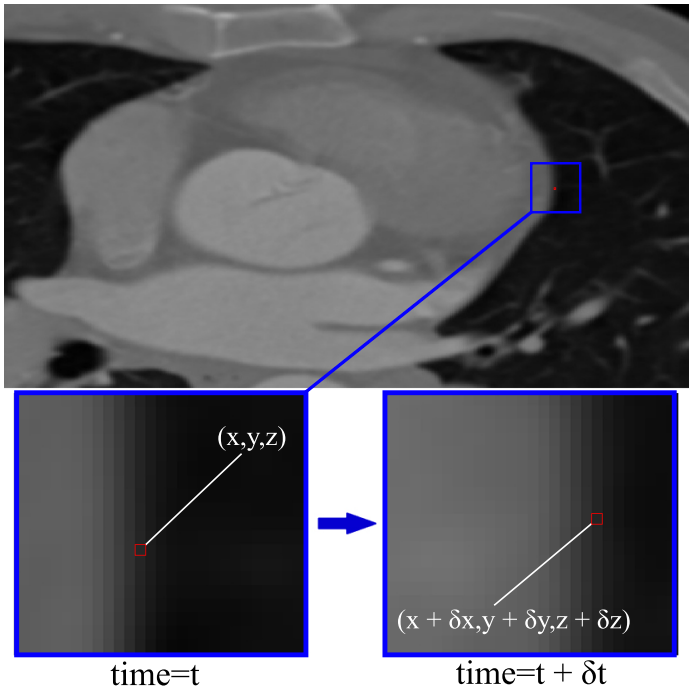

FIGURE 1: TRANSLATION OF A SAMPLE N × N × N CARDIAC WALL REGION BETWEEN TWO CONSECUTIVE TIME POINTS.

a time-dependent analysis. The full equations of motion incorporate acceleration and velocity terms, each contributing distinct forms of energy to the system response. The $[M]\ddot{x}$ term represents the system's inertial force, while the $[K]x$ term depicts the internal elastic forces, corresponding to kinetic and potential energy, respectively. For more realistic modeling, stiffness matrices and force vectors can be nonlinear, more accurately reflecting physical phenomena but increasing model complexity. As a simplification, this system can be modeled as a spring-mass system with an external displacement. The acceleration can then be represented as:

$$\ddot{x} = \frac{[K]}{[M]}(x - u) \tag{6}$$

where u represents the relative displacement of the heart wall and x denotes the displacement of the chest surface. This simplified model provides a foundation for understanding the relationship between cardiac motion and chest surface vibrations while maintaining computational efficiency.

2.3 Computational Domain and FE Model Setup

The computational domain was created by segmenting different organs and tissues from the short-axis CT scan slices. Using the 3D Slicer image computing platform[1], regions of interest were isolated through a segmentation process that defined thresholds to distinguish between tissues and structures based on their density levels. The segmented regions included chest muscles, ribs, cartilage, and lungs (Figure 2a). The software generated a three-dimensional STL model, representing the surface geometry of the segmented structures (Figure 2b). This model was

[1] www.slicer.org/

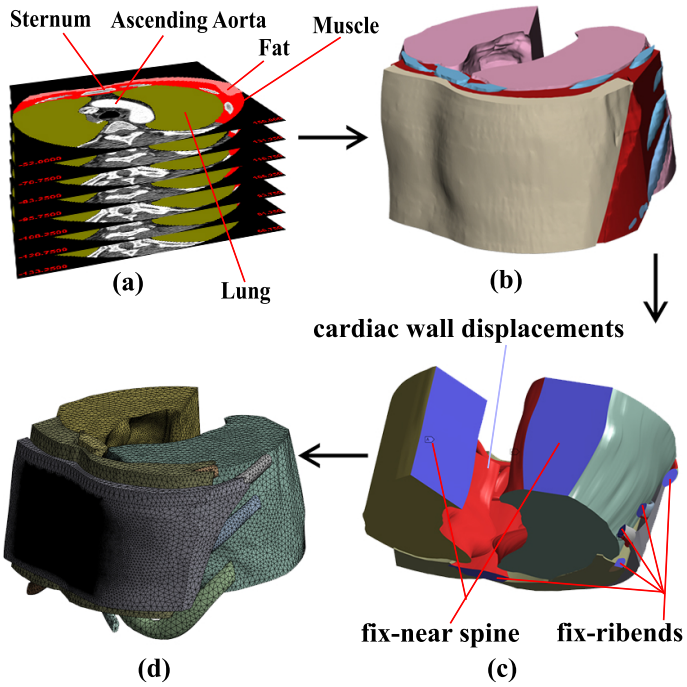

FIGURE 2: OVERVIEW OF THE COMPUTATIONAL MODEL PREPARATION: (A) 4D CT SCAN IMAGES, (B) STL GEOMETRY EXTRACTED FROM CT SCANS, (C) BOUNDARY CONDITIONS, (D) COMPUTATIONAL MESH GENERATION.

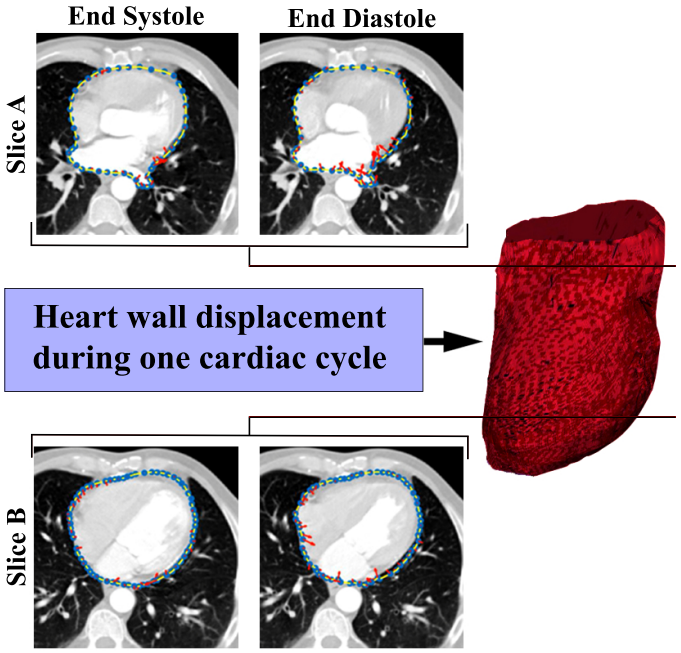

FIGURE 3: EXTRACTING CARDIAC WALL MOTION AS BOUNDARY CONDITIONS FROM 4D CT SCANS. CARDIAC WALL CONTOURS ARE SHOWN IN YELLOW AND THE RED ARROWS INDICATE THE DISPLACEMENT VECTORS. RESULTS ARE SHOWN FOR TWO SAMPLE SLICES AT END OF SYSTOLE AND DIASTOLE.

refined and imported into ANSYS Transient Structural[2]. The heart's location in the 3D geometry was represented by a cavity where displacement boundary conditions extracted from the Lucas-Kanade method were applied. Fixed boundary conditions were set at both ends of the ribs and the posterior side of the lungs, adjacent to the spine (Figure 2c). The structural domain was discretized into tetrahedral mesh elements (Figure 2d), with varying element sizes to ensure mesh independence. This study used linear elastic behavior for tissue materials (Table 1) based on literature values [25–30]. The computational modeling was conducted using the ANSYS Transient Structural analysis module, which utilizes FE method to calculate chest surface acceleration within the computational domain. A time step study was conducted, assuming a cycle duration of 1 second and a sampling frequency of 120 Hz. Simulations employed adaptive step sizes with maximum and minimum time steps of 0.0083 and 0.001 seconds, respectively.

2.4 SCG Signal Processing and Comparison

By solving the equations of motion, the chest surface acceleration map was calculated at a sampling frequency of 120 Hz. To compare the modeled SCG signals with the actual SCG signals acquired by accelerometers, a bandpass filter with cutoff frequencies of 1-30 Hz was employed to remove the low-frequency noise and the higher-frequency chest vibrations. To mitigate potential boundary effects due to filtering, a signal representing 16 cardiac cycles was synthesized by concatenating the original SCG signal. In this study, the dorsoventral SCG component obtained from FE modeling was compared with two actual SCG signals recorded by an accelerometer. The left ventricular (LV) volume was also calculated from CT scan images using 3D Slicer software and compared with the waveforms in the literature (Figure 4, bottom panel).

[2]www.ansys.com

3. RESULTS AND DISCUSSION

Using the Lucas-Kanade method, the complex movements of heart muscles during the cardiac cycle, including rotation, twisting, and longitudinal movement [16], were captured. Capturing these multidimensional movements was important for properly modeling the SCG waveforms at the chest surface. Figure 3 depicts two tracked contours over the heart wall in the short-axis view at two different time instants during a cardiac cycle, i.e., at the and of systole and diastole. The points that were tracked by the Lukas-Kanade method are shown in blue color. These points were carefully selected on the CT images corresponding to the first time point in the 4D data to delineate the boundary around the heart wall. The yellow line represents the curve fitted among these selected points. Red arrows on the contour points show the displacement vectors at each time instant. The arrows have been magnified to eight times their original size to provide a clearer illustration of the displacement vectors. The length and direction of these arrows suggest the displacement and direction of the considered point for the next timestep, respectively.

The LV waveform, representing the cardiac cycle, began at the ECG R peak, corresponding to the beginning of the isovolumic contraction period. The simulated SCG signal was compared with those in Taebi *et al.* (2019) and Inan *et al.* (2014) studies [11,

TABLE 1: MATERIAL PROPERTIES OF THE MODELED TISSUES.

Component	Young's modulus	Density (kg/m^3) [21]	Poisson's ratio [21]
Chest Muscle	2.5 MPa [21, 25]	1000	0.3
Ribcage	12 GPa [21, 26]	2000	0.4
Fat	3.25 kPa [28]	900	0.5
Lung	29 MPa [27, 29]	600	0.45

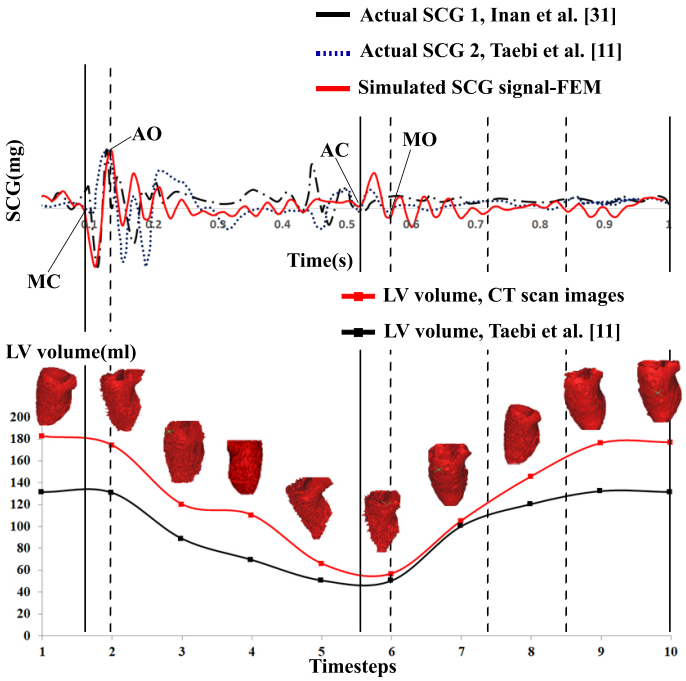

FIGURE 4: (TOP) ACTUAL DORSOVENTRAL SCG DATA FROM [11, 31] VS. SIMULATED SCG USING FE METHOD, AND (BOTTOM) LEFT VENTRICULAR (LV) VOLUME FROM [11] VS. LV VOLUME EXTRACTED FROM THE SUBJECT'S 4D CT SCAN IMAGES IN THE CURRENT STUDY. THE TIME INSTANTS OF THE OPENING AND CLOSURE OF THE AORTIC VALVE (AO AND AC) AND MITRAL VALVE (MO AND MC) ARE SHOWN ON THE SIMULATED SCG SIGNAL.

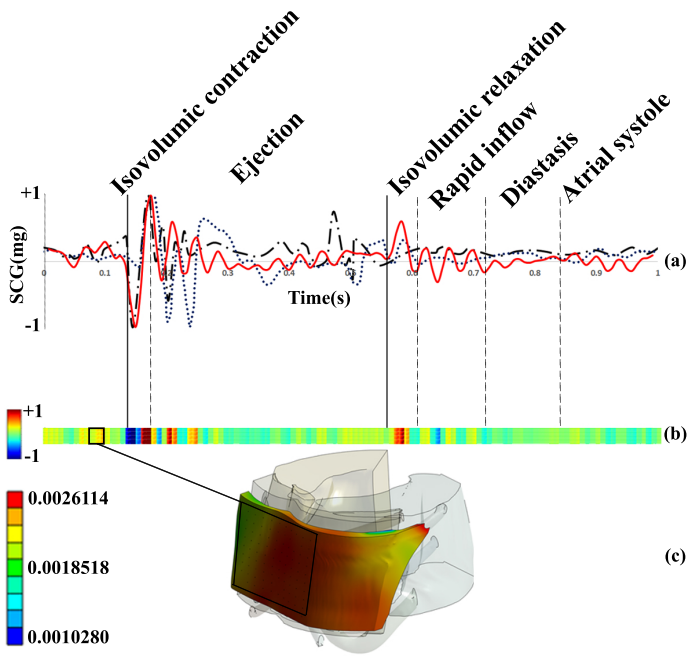

FIGURE 5: DISPLACEMENT HEATMAP COMPARISON WITH THE SIMULATED SCG IN DORSOVENTRAL DIRECTION (A) CARDIAC EVENTS ON SCG GRAPH (B) SNAPSHOTS OF THE DISPLACEMENT HEATMAP, NORMALIZED BETWEEN [-1, 1], DURING A CARDIAC CYCLE. EACH SQUARE CORRESPONDS TO ONE TIME POINT DURING THE CARDIAC CYCLE. (C) AN EXAMPLE OF THE DISPLACEMENT HEATMAP. THE COLORBAR IS SHOWN IN MM AND IS NOT NORMALIZED).

31]. Important cardiac events such as mitral valve closure (MC), AC, and AO were determined based on the LV waveform. The simulated SCG signal exhibited features and fiducial points (AO, AC, and MC) similar to those observed in the SCG waveforms in prior research [21, 32–34]. Figure 5a compares the simulated SCG signal using FE modeling in the dorsoventral direction and Figure 5b the displacement heatmap (normalized between [-1, 1]) of the chest surface generated by employing 100 sensors in the FE simulation results. Moving the rectangle shows the displacement of the chest surface for one cardiac cycle. Figure 5c shows the 3D fat layer from which displacement data was extracted. These findings imply that an FE model could serve as a valuable tool for simulating the transmission of cardiac mechanical motion to the chest surface.

4. LIMITATIONS AND FUTURE WORK

Our current approach presents opportunities for future expansion, including incorporating right-to-left and head-to-foot SCG components. A critical aspect in validating the FE models involves identifying a gold standard signal for comparison with the modeled SCG signals by FE method. In this study, two actual SCG signals from the literature were used and compared with the modeled signals. However, it is well-established that SCG signals exhibit variability across individuals. Therefore, it is crucial to validate the FE results by comparing them with SCG signals obtained from the same participant using gold-standard methods. This can be achieved by simultaneously acquiring actual SCG and CT scan images over multiple cardiac cycles, enhancing the validation of SCG signals from simulations. Additionally, alternative and more realistic material properties and the effects of boundary conditions on outputs can be investigated. While this study focused on analyzing the SCG signal in the dorsoven-

tral direction for one subject, future research aims to increase the sample size and explore SCG signals in all three directions, including the head-to-foot and right-to-left directions.

5. CONCLUSION

This study presents a novel pipeline for modeling SCG signals in the dorsoventral direction using FE analysis. The FE model utilized heart wall displacements extracted from CT scan images as boundary conditions. LV volume was determined from CT scans to interpret SCG data. Key cardiac events, including the timing of heart valve openings and closures, were derived from the combination of LV and SCG waveform. These findings demonstrated consistency with previous studies, validating our methodology. Our results suggest that this personalized FE modeling approach can significantly enhance our understanding of SCG signal generation and propagation through the chest wall. This improved comprehension may lead to more accurate interpretations of SCG data in clinical settings, potentially advancing non-invasive cardiac monitoring techniques.

ACKNOWLEDGMENTS

This work was supported by the National Science Foundation under Grant No. 2340020.

REFERENCES

[1] Mohebi, Reza, Chen, Chen, Ibrahim, Nasrien E, McCarthy, Cian P, Gaggin, Hanna K, Singer, Daniel E, Hyle, Emily P, Wasfy, Jason H and Januzzi Jr, James L. "Cardiovascular disease projections in the United States based on the 2020 census estimates." *Journal of the American College of Cardiology* Vol. 80 No. 6 (2022): pp. 565–578. DOI 10.1016/j.jacc.2022.05.033.

[2] He, Jiang, Ogden, Lorraine G, Bazzano, Lydia A, Vupputuri, Suma, Loria, Catherine and Whelton, Paul K. "Risk factors for congestive heart failure in US men and women: NHANES I epidemiologic follow-up study." *Archives of internal medicine* Vol. 161 No. 7 (2001): pp. 996–1002. DOI 10.1001/archinte.161.7.996.

[3] Gartside, Peter S, Wang, Ping and Glueck, Charles J. "Prospective assessment of coronary heart disease risk factors: the NHANES I epidemiologic follow-up study (NHEFS) 16-year follow-up." *Journal of the American College of Nutrition* Vol. 17 No. 3 (1998): pp. 263–269. DOI 10.1080/07315724.1998.10718757.

[4] Saydah, Sharon, Bullard, Kai McKeever, Cheng, Yiling, Ali, Mohammed K, Gregg, Edward W, Geiss, Linda and Imperatore, Giuseppina. "Trends in cardiovascular disease risk factors by obesity level in adults in the United States, NHANES 1999-2010." *Obesity* Vol. 22 No. 8 (2014): pp. 1888–1895. DOI 10.1002/oby.20761.

[5] Guo, Fangjian and Garvey, W Timothy. "Trends in cardiovascular health metrics in obese adults: National Health and Nutrition Examination Survey (NHANES), 1988–2014." *Journal of the American Heart Association* Vol. 5 No. 7 (2016): p. e003619. DOI 10.1161/JAHA.116.003619.

[6] U.S. Census Bureau. "Population Projections." https://www.census.gov/newsroom/press-releases/2020/population-projections.html (2020). DOI 10.1001/archinte.161.7.996. Accessed: April 29, 2024.

[7] U.S. Census Bureau. "Demographic Turning Points for the United States: Population Projections for 2020 to 2060." https://www.census.gov/content/dam/Census/library/publications/2020/demo/p25-1144.pdf (2020). Accessed: April 29, 2024.

[8] Dehkordi, Parastoo, Khosrow-Khavar, Farzad, Di Rienzo, Marco, Inan, Omer T, Schmidt, Samuel E, Blaber, Andrew P, Sørensen, Kasper, Struijk, Johannes J, Zakeri, Vahid, Lombardi, Prospero et al. "Comparison of different methods for estimating cardiac timings: a comprehensive multimodal echocardiography investigation." *Frontiers in physiology* Vol. 10 (2019): p. 1057. DOI 10.3389/fphys.2019.01057.

[9] Rahman, Mohammad Muntasir, Cook, Jadyn and Taebi, Amirtahà. "Non-contact heart vibration measurement using computer vision-based seismocardiography." *Scientific Reports* Vol. 13 No. 1 (2023): p. 11787. DOI 10.1038/s41598-023-38607-7.

[10] Akhbardeh, Alireza, Tavakolian, Kouhyar, Gurev, Viatcheslav, Lee, Ted, New, William, Kaminska, Bozena and Trayanova, Natalia. "Comparative analysis of three different modalities for characterization of the seismocardiogram." *2009 Annual International Conference of the IEEE Engineering in Medicine and Biology Society*: pp. 2899–2903. 2009. IEEE. DOI 10.1109/IEMBS.2009.5334444.

[11] Taebi, Amirtahà, Solar, Brian E, Bomar, Andrew J, Sandler, Richard H and Mansy, Hansen A. "Recent advances in seismocardiography." *Vibration* Vol. 2 No. 1 (2019): pp. 64–86. DOI 10.3390/vibration2010005.

[12] Gurev, Viatcheslav, Tavakolian, Kouhyar, Constantino, Jason, Kaminska, Bozena, Blaber, Andrew P and Trayanova, Natalia A. "Mechanisms underlying isovolumic contraction and ejection peaks in seismocardiogram morphology." *Journal of medical and biological engineering* Vol. 32 No. 2 (2012): p. 103. DOI 10.5405/jmbe.847.

[13] Korzeniowska-Kubacka, Iwona, Kuśmierczyk-Droszcz, Beata, Bilińska, Maria, Dobraszkiewicz-Wasilewska, Barbara, Mazurek, Krzysztof and Piotrowicz, Ryszard. "Seismocardiography—a non-invasive method of assessing systolic and diastolic left ventricular function in ischaemic heart disease." *Cardiology Journal* Vol. 13 No. 4 (2006): pp. 319–325. URL https://journals.viamedica.pl/cardiology_journal/article/view/21817.

[14] Cook, Jadyn, Umar, Muneebah, Khalili, Fardin and Taebi, Amirtahà. "Body acoustics for the non-invasive diagnosis of medical conditions." *Bioengineering* Vol. 9 No. 4 (2022): p. 149. DOI 10.3390/bioengineering9040149.

[15] Taebi, Amirtaha. "Characterization, classification, and genesis of seismocardiographic signals." (2018)URL http://purl.fcla.edu/fcla/etd/CFE0007106.

[16] Scott, Andrew D, Keegan, Jennifer and Firmin, David N. "Motion in cardiovascular MR imaging." *Radiology* Vol. 250 No. 2 (2009): pp. 331–351. DOI 10.1148/radiol.2502071998.

[17] Crow, Richard S, Hannan, Peter, Jacobs, David, Hedquist, Lowell and Salerno, David M. "Relationship between seismocardiogram and echocardiogram for events in the cardiac cycle." *American journal of noninvasive cardiology* Vol. 8 No. 1 (1994): pp. 39–46. DOI 10.1159/000470156.

[18] Giorgis, Lionel, Hernandez, Alfredo I, Amblard, Amel, Senhadji, Lotfi, Cazeau, Serge, Jauvert, Gaël and Donal, Erwan. "Analysis of cardiac micro-acceleration signals for the estimation of systolic and diastolic time intervals in cardiac resynchronization therapy." *2008 Computers in Cardiology*: pp. 393–396. 2008. IEEE. DOI 10.1109/CIC.2008.4749061.

[19] Mann, Aysha, Thibbotuwawa Gamage, Peshala, Kakavand, Bahram and Taebi, Amirtahà. "Exploring the impact of sensor location on seismocardiography-derived cardiac time intervals." *Journal of Engineering and Science in Medical Diagnostics and Therapy* (2024): pp. 1–19DOI 10.1115/1.4063203.

[20] Gamage, Peshala T, Azad, Md Khurshidul, Sandler, Richard H and Mansy, Hansen A. "Modeling Seismocardiographic signal using finite element Modeling and medical image processing." *2019 IEEE Signal Processing in Medicine and Biology Symposium (SPMB)*: pp. 1–4. 2019. IEEE. DOI 10.1109/SPMB47826.2019.9037842.

[21] Gamage, Peshala Priyadarshana Thibbotuwawa. "Seismocardiography-Genesis, And Utilization of Machine Learning for Variability Reduction and Improved Cardiac Health Monitoring." Ph.D. Thesis, University of Central Florida. 2020. URL https://stars.library.ucf.edu/etd2020/622/.

[22] Sandler, Richard H, Hassan, Tanvir, Rahman, Badrun, Gamage, Peshala and Mansy, Hansen. "Effect Of Extra Soft Tissue On Seismocardiographic Signal Using Finite Element Analysis." *Journal of Cardiac Failure* Vol. 29 No. 4 (2023): p. 599. DOI 10.1016/j.cardfail.2022.10.132.

[23] Mithani, Sahil, Wang, Juntao, Diarra, Zeinabou, Lin, David J and Inan, Omer T. "Finite Element Modeling of the Infant Heart to Determine the Relationship between Single Ventricle Disease and the Seismocardiogram." *2022 Opportunity Research Scholars Symposium (ORSS)*: pp. 57–61. 2022. IEEE. DOI 10.1109/ORSS55359.2022.9806035.

[24] Lucas, Bruce D and Kanade, Takeo. "An iterative image registration technique with an application to stereo vision." *IJCAI'81: 7th international joint conference on Artificial intelligence*, Vol. 2: pp. 674–679. 1981. URL https://hal.science/hal-03697340/.

[25] Chawla, A, Mukherjee, S and Karthikeyan, B. "Characterization of human passive muscles for impact loads using genetic algorithm and inverse finite element methods." *Biomechanics and modeling in mechanobiology* Vol. 8 (2009): pp. 67–76. DOI 10.1007/s10237-008-0121-6.

[26] Gefen, Amit and Dilmoney, Benny. "Mechanics of the normal woman's breast." *Technology and Health Care* Vol. 15 No. 4 (2007): pp. 259–271. DOI 10.3233/THC-2007-15404.

[27] Grimal, Quentin, Gama, Bazle A, Naili, Salah, Watzky, Alexandre and Gillespie Jr, John W. "Finite element study of high-speed blunt impact on thorax: linear elastic considerations." *International journal of impact engineering* Vol. 30 No. 6 (2004): pp. 665–683. DOI 10.1016/j.ijimpeng.2003.08.002.

[28] Sims, Aaron M, Stait-Gardner, T, Fong, L, Morley, John W, Price, William S, Hoffman, M, Simmons, Anne and Schindhelm, Klaus. "Elastic and viscoelastic properties of porcine subdermal fat using MRI and inverse FEA." *Biomechanics and modeling in mechanobiology* Vol. 9 (2010): pp. 703–711. DOI 10.1007/s10237-010-0207-9.

[29] Sundaram, SH. "Finite element analysis of the human thorax." *J Biomech* Vol. 10 (1988): pp. 227–241. DOI 10.1016/0021-9290(77)90104-X.

[30] Zigras, Tiffany C, Nagano, Naoko, Tremblay, Dominique, Rouleau, Leonie, Mongrain, Rosaire, Cartier, Raymond and Leask, Richard L. "Biaxial Testing of Human Pericardium: A Comparative Study of Fixed and Fresh Tissue." *Summer Bioengineering Conference*, Vol. 47985: pp. 199–200. 2007. American Society of Mechanical Engineers. DOI 10.1115/SBC2007-176424.

[31] Inan, Omer T, Migeotte, Pierre-Francois, Park, Kwang-Suk, Etemadi, Mozziyar, Tavakolian, Kouhyar, Casanella, Ramon, Zanetti, John, Tank, Jens, Funtova, Irina, Prisk, G Kim et al. "Ballistocardiography and seismocardiography: A review of recent advances." *IEEE journal of biomedical and health informatics* Vol. 19 No. 4 (2014): pp. 1414–1427. DOI 10.1109/JBHI.2014.2361732.

[32] Mann, Aysha J, Kakavand, Bahram, Thibbotuwawa Gamage, Peshala and Taebi, Amirtahà. "Effect of Measurement Location on Cardiac Time Intervals Estimated by Seismocardiography." *ASME International Mechanical Engineering Congress and Exposition*, Vol. 87622: p. V005T06A070. 2023. American Society of Mechanical Engineers. DOI 10.1115/IMECE2023-112702.

[33] Mann, Aysha, Rahman, Mohammad Muntasir, Vanga, Vineeth, Thibbotuwawa Gamage, Peshala and Taebi, Amirtahà. "Variation of Seismocardiogram-Derived Cardiac Time Intervals and Heart Rate Variability Metrics Across the Sternum." *Journal of Medical Devices* (2024).

[34] Rahman, Mohammad Muntasir, Mann, Aysha J and Taebi, Amirtahà. "ECG-Free Assessment of Cardiac Valve Events Using Seismocardiography." *IEEE Body Sensor Networks*. 2024. IEEE.